

# Structure-Based Design of Tetrahydroisoquinoline-7-carboxamides as Selective Discoidin Domain Receptor 1 (DDR1) Inhibitors

Zhen Wang,<sup>†,‡</sup> Huan Bian,<sup>||</sup> Sergio G. Bartual,<sup>⊥</sup> Wenting Du,<sup>#</sup> Jinfeng Luo,<sup>†</sup> Hu Zhao,<sup>||</sup> Shasha Zhang,<sup>†</sup> Cheng Mo,<sup>†,‡</sup> Yang Zhou,<sup>†,‡</sup> Yong Xu,<sup>†</sup> Zhengchao Tu,<sup>†</sup> Xiaomei Ren,<sup>†</sup> Xiaoyun Lu,<sup>†,§</sup> Rolf A. Brekken,<sup>#</sup> Libo Yao,<sup>||</sup> Alex N. Bullock,<sup>\*,⊥</sup> Jin Su,<sup>\*,||</sup> and Ke Ding<sup>\*,†,§</sup>

<sup>†</sup>State Key Laboratory of Respiratory Diseases, Guangzhou Institutes of Biomedicine and Health, Chinese Academy of Sciences, 190 Kaiyuan Avenue, Guangzhou 510530, China

<sup>‡</sup>University of the Chinese Academy of Sciences, 19 Yuquan Road, Beijing 100049, China

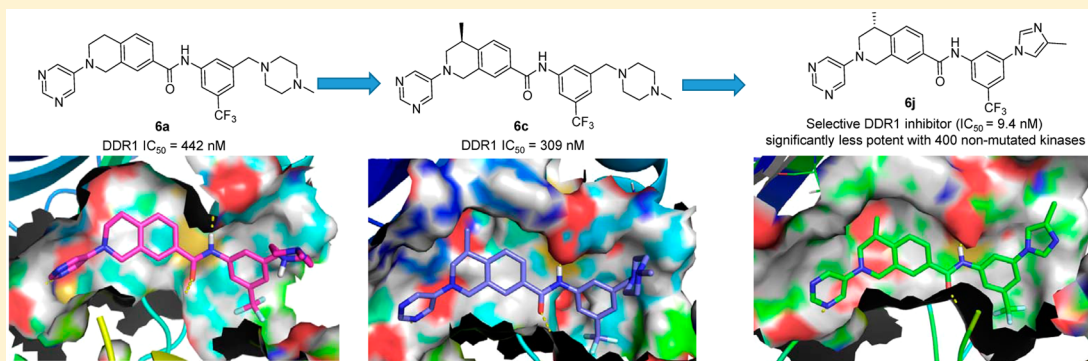
<sup>§</sup>School of Pharmacy, Jinan University, 601 Huangpu Avenue West, Guangzhou 510632, China

<sup>||</sup>Department of Biochemistry and Molecular Biology, The Fourth Military Medical University, 17 Changle Western Road, Xi'an, Shaanxi 710032, P. R. China

<sup>⊥</sup>Structural Genomics Consortium, University of Oxford, Old Road Campus, Roosevelt Drive, Oxford OX3 7DQ, U.K.

<sup>#</sup>Division of Surgical Oncology, Department of Surgery and the Hamon Center for Therapeutic Oncology Research, UT Southwestern Medical Center, Dallas Texas 75390-8593, United States

## Supporting Information



**ABSTRACT:** The structure-based design of 1, 2, 3, 4-tetrahydroisoquinoline derivatives as selective DDR1 inhibitors is reported. One of the representative compounds, **6j**, binds to DDR1 with a  $K_d$  value of 4.7 nM and suppresses its kinase activity with an  $IC_{50}$  value of 9.4 nM, but it is significantly less potent for a panel of 400 nonmutated kinases. **6j** also demonstrated reasonable pharmacokinetic properties and a promising oral therapeutic effect in a bleomycin-induced mouse pulmonary fibrosis model.

## INTRODUCTION

Discoidin domain receptors (i.e., DDR1 and DDR2) are transmembrane receptor tyrosine kinases (RTKs) that specifically recognize fibrillar collagens as extracellular ligands.<sup>1–3</sup> DDR1 and DDR2 are highly involved in fundamental cellular processes, including cell proliferation, migration, adhesion, and matrix remodeling.<sup>4–11</sup> The dysregulation of DDR1 has been linked to a variety of human cancers and inflammatory conditions such as fibrotic disorders and atherosclerosis.<sup>4–11</sup> Collective evidence indicates a critical link between DDR1 and pulmonary fibrosis, a lethal disease with few therapeutic options.<sup>6,8,11,12</sup> For instance, a DDR1 deletion has been reported to alleviate bleomycin (BLM)-induced lung inflammation and pulmonary fibrosis by blocking P38 mitogen-activated protein kinase (p38 MAPK) activation.<sup>12</sup>

We and others have identified several classes of DDR1 inhibitors with different selectivity profiles and have demonstrated their therapeutic potential for various human cancers (Figure 1).<sup>13–18,28</sup> However, these small molecules still have relatively poor target specificity and there are limited reports on the efficacy of the pharmacologic inhibition of DDR1 in models of pulmonary fibrosis.<sup>8</sup> In this article, we report the structure-based design of tetrahydroisoquinoline derivatives as new highly selective DDR1 inhibitors with promising therapeutic effects in a BLM-induced pulmonary fibrosis mouse model.

**Received:** January 29, 2016

**Published:** May 24, 2016



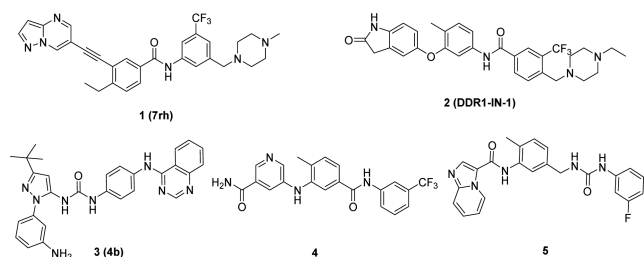


Figure 1. Selective DDR1/DDR2 kinase inhibitors.

## RESULTS AND DISCUSSION

DDR1 shares approximately 61% sequence identity with Abelson (Abl) kinase in its adenosine triphosphate (ATP) binding domain, and most reported selective DDR1 inhibitors are derivatized from Abl antagonists.<sup>19</sup> Previous investigations revealed that a  $\pi$ - $\pi$  stacking interaction between the chemical molecule and Tyr<sup>253</sup> of Abl is critical for most of the reported Abl inhibitors (Supporting Information (SI), Figure S1A,B,C),<sup>20–22</sup> but the corresponding interaction is unnecessary for DDR1 binding. Indeed, DDR1-IN-1 achieved selective DDR1 inhibition because its hinge binding moiety is oriented away from the P-loop, avoiding the potential  $\pi$ - $\pi$  interactions with Tyr<sup>253</sup> in Abl.<sup>23</sup> However, the molecule could form an additional  $\pi$ - $\pi$  interaction with Phe<sup>382</sup> in Abl, which contributed greatly to its relatively low selectivity between DDR1 and Abl (SI, Figure S1D).<sup>21,22</sup> Diminishing this interaction may further improve DDR1 selectivity. On the basis of this hypothesis, a series of 1, 2, 3, 4-tetrahydroisoquinoline derivatives were designed as novel, selective DDR1 inhibitors in which a pyrimidinyl group was utilized as the potential hinge binding moiety. A *N*-(3-((4-methylpiperazin-1-yl)methyl)-5-(trifluoromethyl)phenyl)carboxamide group was also introduced based on our previous investigation (Figure 2A).<sup>13</sup>

Our preliminary modeling suggested that the initial lead, **6a**, could fit nicely into the DDR1 binding pocket and maintain the key interactions with DDR1. The pyrimidinyl moiety of **6a** could form an essential hydrogen bond with the NH of Met<sup>704</sup> in the hinge region of DDR1. Two additional hydrogen bonds have also formed between the linker amide and Glu<sup>672</sup> in the C-helix and Asp<sup>784</sup> in the Asp-Phe-Gly (DFG) motif, respectively (Figure 2B). Encouragingly, compound **6a** failed to dock into the Abl binding pocket, suggesting its potential selectivity among kinases. Compound **6a** and its derivatives were readily synthesized using Buchwald–Hartwig amination as the key step (Scheme 1).<sup>24</sup> Briefly, the substituted methyl 4-(2-(2,2,2-trifluoroacetamido)ethyl)benzoate (**8**) was prepared by the trifluoroacetylation of methyl 4-(2-aminoethyl)benzoate (**7**) and then underwent a classical Pictet–Spengler reaction to yield the protected tetrahydroisoquinoline derivatives (**9**), which were deprotected and reacted with a hydrochloric acid solution in MeOH to form the key intermediate (**10**). Compound **10** was coupled with 5-bromopyrimidine, 3-bromopyridine, or bromobenzene through a Buchwald–Hartwig amination reaction to provide compound **11**. The final products were obtained by treating intermediate **11** with different anilines under basic conditions.

DDR1 inhibition of the compounds was determined using a well-established Lance Ultra kinase assay.<sup>25</sup> The potential target selectivity was additionally evaluated by monitoring their inhibition against Abl. Compound **1** was included as a positive

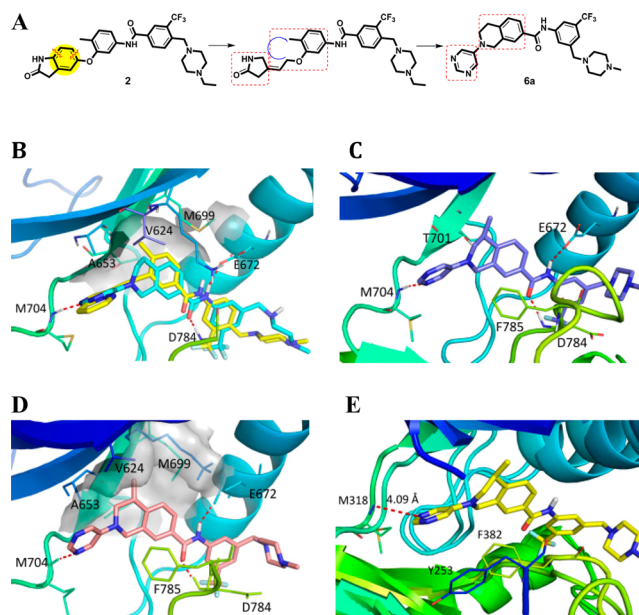
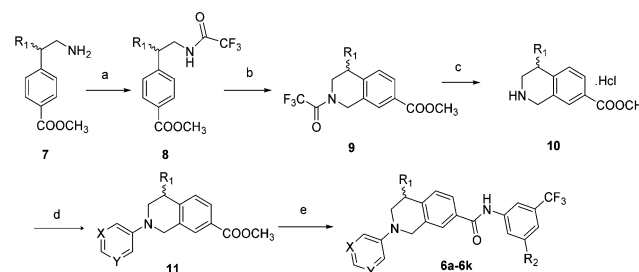


Figure 2. (A) Design of new DDR1 inhibitor **6a**. (B) Molecular docking of **6a** (cyan) into the DDR1-ponatinib (yellow) costructure (PDB ID: 3ZOS). (C) Co-crystal structure of **6c** with DDR1 (PDB ID: 5FDP). (D) Molecular docking of **6b** into DDR1. (E) Superposition of **6c** with Abl (PDB ID: 3IK3).

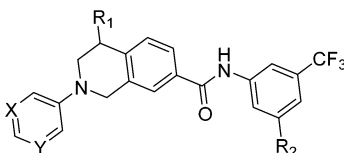
## Scheme 1. Synthesis of Compound **6a** and its Derivatives<sup>a</sup>



<sup>a</sup>Reagents and conditions: (a) trifluoroacetic anhydride, 0 °C to rt, 58–63%; (b) (HCHO)<sub>m</sub>, conc H<sub>2</sub>SO<sub>4</sub>, 0 °C to rt, 51–89%; (c) (i) K<sub>2</sub>CO<sub>3</sub>, MeOH/H<sub>2</sub>O (2:1), rt, (ii) HCl·MeOH, MeOH, rt, 86–95% (two steps); (d) 5-bromopyrimidine or 3-bromopyridine or bromobenzene, Pd(dba)<sub>2</sub>, Ruphos, Cs<sub>2</sub>CO<sub>3</sub>, toluene, 80 °C, 42–89%; (e) substituted aniline, *t*-BuOK, THF, –20 °C to rt, 69–86%.

control, which displayed similar IC<sub>50</sub> values to the previously reported data.<sup>13</sup> It was shown that **6a** exhibited modest DDR1 inhibitory activity, with an IC<sub>50</sub> value of 442 nM, while its potency against Abl was strikingly inferior (IC<sub>50</sub> > 10.0  $\mu$ M). These results are consistent with our computational prediction.

Further computational investigation suggested that a small hydrophobic recess formed by Val<sup>624</sup>, Ala<sup>653</sup>, and Met<sup>699</sup> was available in the ATP binding pocket of DDR1 (Figure 2B). A lipophilic substituent at R<sub>1</sub> may occupy this pocket to achieve improved potency. The (*R*)-methyl (**6b**) and (*R*)-ethyl derivatives (**6d**) displayed a 20-fold and 12-fold potency improvement, respectively. The (*S*)-methyl compound (**6c**), in which the methyl moiety was oriented away from the pocket, as confirmed by a 2.3 Å cocrystal structure with DDR1 (Figure 2C), displayed a similar inhibitory potency to that of the R<sub>1</sub> unsubstituted **6a**. A large group at the R<sub>1</sub> position was predicted to be detrimental to the binding of DDR1. As expected, R<sub>1</sub>-(*R*)-isopropyl (**6f**) caused a substantial potency

Table 1. In Vitro Kinase Inhibition of Compounds 6a–6k against DDR1<sup>a</sup> and Abl1<sup>b</sup>


compd	X	Y	R <sub>1</sub>	R <sub>2</sub>	kinase inhibition (IC <sub>50</sub> , nM)	
					DDR1	Abl1
6a	N	N	H	(4-methylpiperazin-1-yl)methyl	442 ± 69	>10000
6b	N	N	(R)-Me	(4-methylpiperazin-1-yl)methyl	24.3 ± 4.1	>10000
6c	N	N	(S)-Me	(4-methylpiperazin-1-yl)methyl	309 ± 44	>10000
6d	N	N	(R)-Et	(4-methylpiperazin-1-yl)methyl	36.4 ± 5.7	>10000
6e	N	N	(S)-Et	(4-methylpiperazin-1-yl)methyl	>2000	>10000
6f	N	N	(R)-i-Pr	(4-methylpiperazin-1-yl)methyl	>1000	>10000
6g	N	N	(S)-i-Pr	(4-methylpiperazin-1-yl)methyl	>3000	>10000
6h	N	C	H	(4-methylpiperazin-1-yl)methyl	328 ± 35	>10000
6i	C	C	H	(4-methylpiperazin-1-yl)methyl	>3000	>10000
6j	N	N	(R)-Me	4-methyl-1H-imidazol-1-yl	9.4 ± 1.7	>10000
6k	N	N	(S)-Me	4-methyl-1H-imidazol-1-yl	326 ± 43	>10000
1 <sup>13</sup>					9.7 ± 2.3	308 ± 42

<sup>a</sup>DDR1 experiments were performed using the LANCE ULTRA kinase assay, according to the manufacturer's instructions. The data are the means from at least two independent experiments. <sup>b</sup>Abl1 activity experiments were performed using the FRET-based Z-Lyte assay, according to the manufacturer's instructions. The data are the means from at least 3 independent experiments.

Table 2. Pharmacokinetic Profile of Compound 6j in Mice<sup>a</sup> and Rats<sup>b</sup>

	mice		rats	
	oral 4 mg/kg	iv 1 mg/kg	oral 20 mg/kg	iv 4 mg/kg
AUC <sub>(0–∞)</sub> (ng/mL·h)	2554.1	1211.9	788.3 ± 41.5	236.0 ± 53.1
T <sub>1/2</sub> (h)	1.1	0.2	1.3 ± 0	1.5 ± 0.3
T <sub>max</sub> (h)	0.5		1 ± 0	
C <sub>max</sub> (ng/mL)	2193.9	2246.8	341.7 ± 115.5	473.3 ± 114.7
CL <sub>z</sub> (L/h/kg)		0.8		17.6 ± 4.4
BA (%)	41.6		66.8	

<sup>a</sup>ICR mice (male, 24 animals per group) weighing 18–30 g were used for the study. <sup>b</sup>SD rats (male, 3 animals per group) weighing 180–220 g were used for the study.

loss for DDR1. Additionally, compounds **6e** and **6g**, which featured (S)-ethyl and (S)-isopropyl, respectively, displayed almost no DDR1 inhibition. The X-ray crystal structure also confirmed the presence of a strong hydrogen bonding network between the new inhibitor and DDR1 (Figure 2C). The deletion of a hydrogen bond by eliminating the N atoms in the pyrimidinyl group (**6i**) totally abolished DDR1 inhibitory potency. Not surprisingly, when the pyrimidinyl group was replaced by a pyridinyl moiety, the resulting compound, **6h**, exhibited an almost identical IC<sub>50</sub> value to that of **6a**.

It was also noteworthy that all the new DDR1 inhibitors exhibited excellent DDR1 selectivity over the structurally related Abl kinase (Table 1). To rationalize this target selectivity, the inhibitor **6c** was superimposed into the Abl structure (PDB ID: 3IK3) (Figure 2E). It was shown that the 1, 2, 3, 4-tetrahydroisoquinoline scaffold in **6c** forced the pyrimidinyl moiety to adopt a different dihedral angle that prevented the formation of critical interactions with Tyr<sup>253</sup> and Phe<sup>382</sup> in Abl. Moreover, the distance between the N atom in the pyrimidinyl group and Met<sup>318</sup> in Abl was predicted to be 4.09 Å, which exceeds the limit to form a potential hydrogen bond.

Further structural optimization of the inhibitor **6b** yielded **6j** as a promising candidate, with an IC<sub>50</sub> value of 9.4 nM against

DDR1 (Table 1). The compound also exhibited reasonable pharmacokinetic (PK) properties, with an oral bioavailability of 66.8% and a T<sub>1/2</sub> value of 1.25 h at an oral dose of 20 mg/kg (Table 2) in rats. The PK profile of compound **6j** was also investigated in ICR mice, which showed that the compound had a similar oral bioavailability to that of rats. However, the area under concentration–time curve (AUC) value of the compound in mice was obviously higher than that in rats, suggesting its good absorption property in mice.

The DDR1 inhibition of **6j** was further validated by determining its binding affinity with the DDR1 protein (conducted by DiscoverX, San Diego, CA).<sup>26</sup> It was shown that **6j** bound tightly to DDR1, with a binding constant (K<sub>d</sub>) value of 4.7 nM. The target specificity of **6j** was also investigated by conducting a kinase selectivity profiling study against a panel of 468 kinases (including 403 nonmutated kinases) at 1.0 μM, which is approximately 210-fold above its K<sub>d</sub> value against DDR1 using the DiscoverX screening platform. It was shown that **6j** displayed excellent target selectivity, with S(10) and S(1) scores of 0.022 and 0.012, respectively (Table S5).<sup>26</sup> The potential “off-target” kinases tested included cyclin-dependent kinase 11 (CDK 11), DDR2, ephrin type-B receptor 8 (EPHB8), muscle-specific receptor tyrosine kinase (MUSK), nerve growth factor receptor A



(TrkA), TrkB, and TrkC. However, the  $IC_{50}$  value of **6j** against DDR2 was determined to be 188 nM in our Lance Ultra kinase assay, indicating that **6j** was 20-fold less potent against DDR2. Further determination of the binding affinities ( $K_d$  values) revealed that **6j** exhibited an approximately 21–120-fold less potency against the majority of the other “off target” kinases, with the exception of TrkB and TrkC, which displayed  $K_d$  values of 22 and 18 nM, respectively (Figure 3). These results collectively supported the extraordinary target selectivity of **6j** against DDR1.

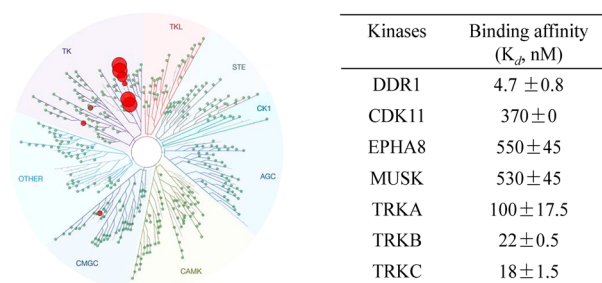


**Figure 3.** (A) KinomeScan kinase selectivity profiles for **6j**. Compound **6j** was profiled at a concentration of  $1.0 \mu\text{M}$  against a diverse panel of 468 kinases by DiscoverX. (B) Binding constants ( $K_d$  values) of compound **6j** against the top hits. The data are the means from at least three independent experiments.

Further investigation revealed that the activation of DDR1 as well as its downstream signaling intermediate, p38,<sup>27</sup> were both dose-dependently suppressed by **6j** in primary human lung fibroblasts (Figure 4), suggesting the efficacy of this compound

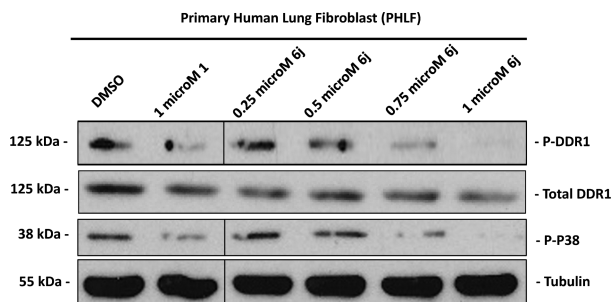


**Figure 4.** Effects of DDR1 inhibition by **6j** on signaling in primary human lung fibroblasts. **6j** inhibited DDR1-mediated signaling in a concentration-dependent manner in primary human lung fibroblasts (24 h treatment). Lysates were probed for the indicated targets by Western blot analysis.

against DDR1-induced signaling. In light of the critical role of DDR1 in BLM-induced pulmonary fibrosis,<sup>12</sup> we treated mice with compound **6j** after the onset of a BLM challenge. Inhibitor **6j** was orally administered at 10 and 50 mg/kg twice daily (BID) for 2 weeks based on its PK properties (Table 2). Unlike those from the phosphate buffered saline (PBS) treated mice, which had large alveolar spaces and were weakly stained by Masson's trichrome, the lungs from BLM-challenged animals exhibited a reduction in alveolar spaces and were stained blue by Masson's trichrome, demonstrating typical fibrotic features. The compound prevented these BLM-induced pathological changes in a dose-dependent manner (Figure 5A). These results agreed with the expression levels of fibrotic markers in lung tissue lysates, including fibronectin and  $\alpha$ -smooth muscle

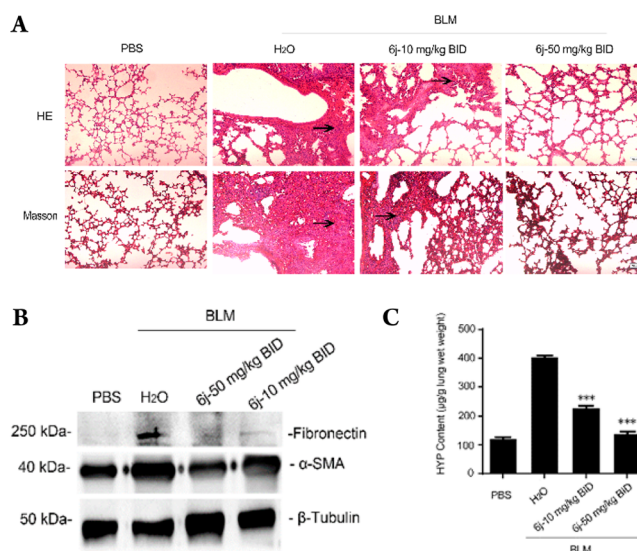


**Figure 5.** Compound **6j** prevents BLM-induced lung fibrosis. Fourteen days after the onset of BLM injury, C57BL/6 mice (five animals each group) received an oral gavage of **6j** twice daily at the indicated dosages, and the lungs were collected on day 28. The upper panels in (A) display the hematoxylin and eosin (H&E) staining images of the dissected lungs. The bottom panels in (A) represent Masson's trichrome staining. The arrows indicate the fibrotic areas of the tissues. The images in (B) show the results of the immunoblotting with the indicated antibodies. The histogram in (C) shows the determined hydroxyproline content. \*\*\* $P < 0.001$ .

actin (SMA) (Figure 5B).<sup>28</sup> Further analyses also revealed that the administration of compound **6j** caused a dose-dependent suppression in the content of hydroxyproline (Figure 5C), a unique amino acid found in collagen.<sup>29</sup> The above data collectively indicate the promising therapeutic potential of **6j** against the BLM-induced pulmonary fibrosis.

## CONCLUSION

In summary, a series of 1, 2, 3, 4-tetrahydroisoquinoline derivatives were designed as novel highly selective DDR1 inhibitors. Compound **6j** strongly suppressed DDR1, with a single digit nM  $IC_{50}$  value, but it is significantly less potent in a panel of 400 nonmutated kinases. Thus, to the best of our knowledge, this compound represents one of the most selective DDR1 inhibitors to date. The compound also demonstrated reasonable PK properties and a promising oral therapeutic effect in a BLM-induced mouse pulmonary fibrosis model. Its strong DDR1 inhibitory potency and extraordinary target specificity make compound **6j** not only a promising lead compound for new drug discovery but also a valuable research probe for further biological investigation of its target.

## EXPERIMENTAL SECTION

**General Chemistry.** Reagents and solvents were obtained from commercial suppliers and used without further purification. Flash chromatography was performed using silica gel (200–300 mesh).  $^1\text{H}$  and  $^{13}\text{C}$  NMR spectra were recorded on a Bruker AV-400 spectrometer at 400 MHz and Bruker AV-500 spectrometer at 125 MHz. The low or high resolution of ESI-MS was recorded on an Agilent 1200 HPLC-MSD mass spectrometer or Applied Biosystems Q-STAR Elite ESI-LC-MS/MS mass spectrometer, respectively. The purity of compounds was determined to be over 95% (>95%) by reverse-phase high performance liquid chromatography (HPLC) analysis. HPLC instrument: Dionex Summit HPLC (column,

Diamonsil C18, 5.0  $\mu\text{m}$ , 4.6 mm  $\times$  250 mm (Dikma Technologies); detector, PDA-100 photodiode array; injector, ASI-100 autoinjector; pump, p-680A). Elution: 85% MeOH in water with 0.1% modifier (ammonia, v/v); flow rate, 1.0 mL/min.

## ■ ASSOCIATED CONTENT

### Supporting Information

The Supporting Information is available free of charge on the ACS Publications website at DOI: 10.1021/acs.jmedchem.6b00140.

Synthetic procedures and compound characterization, procedures, and results for in vitro kinase assay, KINOMEscan, protein expression and purification, crystallization and structure determination, computational study, Western blot analysis, animal experiments, antitumor activity of compound **6j**. The  $^1\text{H}$  and  $^{13}\text{C}$  NMR spectra of compounds **6a–6k** (PDF)  
Molecular formula strings (CSV)

### Accession Codes

Atomic coordinates and experimental data for the co-crystal structure of **6c** with DDR1 (PDB ID: SFDP) will be released upon article publication.

## ■ AUTHOR INFORMATION

### Corresponding Authors

\*For A.N.B.: E-mail, alex.bullock@sgc.ox.ac.uk.

\*For J.S.: E-mail, sujin923@fmmu.edu.cn.

\*For K.D.: phone, +86-20-32015276; fax, +86-20-32015299; E-mail, ding\_ke@gibh.ac.cn.

### Author Contributions

Z. Wang, H. Bian, and S. G. Bartual contributed equally to this work.

### Notes

The authors declare no competing financial interest.

## ■ ACKNOWLEDGMENTS

We appreciate the financial support from the National Natural Science Foundation of China (81425021 and 21572230) and the Natural Science Foundation of Guangdong Province (2015A03031201). We also thank Diamond Light Source for beam time (proposal mx8421) as well as the staff of beamline I04 for their assistance with crystal testing and data collection. The SGC is a registered charity (no. 1097737) that receives funds from AbbVie, Bayer Pharma AG, Boehringer Ingelheim, the Canada Foundation for Innovation, the Eshelman Institute for Innovation, Genome Canada, Innovative Medicines Initiative (EU/EFPIA) [ULTRA-DD grant no. 115766], Janssen, Merck & Co., Novartis Pharma AG, Ontario Ministry of Economic Development and Innovation, Pfizer, São Paulo Research Foundation-FAPESP, Takeda, and Wellcome Trust [092809/Z/10/Z].

## ■ ABBREVIATIONS USED

DDR, discoidin domain receptor;  $\text{IC}_{50}$ , half-maximal (50%) inhibitory concentration of a substance; RTKs, receptor tyrosine kinases; p38 MAPK, P38 mitogen-activated protein kinase; Abl, abelson; ATP, adenosine triphosphate; Tyr, tyrosine; Phe, phenylalanine; Met, methionine; Glu, glutamic acid; Asp, aspartic acid; DFG, Asp-Phe-Gly; MeOH, methanol; PDB, Protein Data Bank; rt, room temperature; Pd(dba)<sub>2</sub>, bis(dibenzylideneacetone)palladium; Ruphos, 2-dicyclohexyl phosphino-2',6'-diisopropoxy-1,1'-biphenyl; *t*-BuOK, potassi-

um *tert*-butanolate; THF, tetrahydrofuran; Val, valine; Ala, alanine; compd, compounds; AUC, area under concentration–time curve;  $T_{1/2}$ , half-life period; ICR, Institute of Cancer Research; SD, Sprague–Dawley;  $T_{\text{max}}$ , peak time;  $C_{\text{max}}$ , peak concentration; CL, clearance; BA, bioavailability; iv, intravenous; CDK11, cyclin-dependent kinase 11; EPHB8, ephrin type-B receptor 8; MUSK, muscle-specific receptor tyrosine kinase; TrkA, nerve growth factor receptor A; PHLF, primary human lung fibroblast; BLM, bleomycin; BID, twice daily; PK, pharmacokinetic; PBS, phosphate buffered saline; SMA,  $\alpha$ -smooth muscle actin; H&E, hematoxylin and eosin

## ■ REFERENCES

- (1) Shrivastava, A.; Radziejewski, C.; Campbell, E.; Kovac, L.; McGlynn, M.; Ryan, T. E.; Davis, S.; Goldfarb, M. P.; Glass, D. J.; Lemke, G.; Yancopoulos, G. D. An orphan receptor tyrosine kinase family whose members serve as nonintegrin collagen receptors. *Mol. Cell* **1997**, *1*, 25–34.
- (2) Vogel, W.; Gish, G. D.; Alves, F.; Pawson, T. The discoidin domain receptor tyrosine kinases are activated by collagen. *Mol. Cell* **1997**, *1*, 13–23.
- (3) Xu, H.; Raynal, N.; Stathopoulos, S.; Myllyharju, J.; Farndale, R. W.; Leiting, B. Collagen binding specificity of the discoidin domain receptors: binding sites on collagens II and III and molecular determinants for collagen IV recognition by DDR1. *Matrix Biol.* **2011**, *30*, 16–26.
- (4) Vogel, W. F.; Abdulhussein, R.; Ford, C. E. Sensing extracellular matrix: an update on discoidin domain receptor function. *Cell. Signalling* **2006**, *18*, 1108–1116.
- (5) Valiathan, R. R.; Marco, M.; Leiting, B.; Kleer, C. G.; Fridman, R. Discoidin domain receptor tyrosine kinases: new players in cancer progression. *Cancer Metastasis Rev.* **2012**, *31*, 295–321.
- (6) Leiting, B. Discoidin domain receptor functions in physiological and pathological conditions. *Int. Rev. Cell Mol. Biol.* **2014**, *310*, 39–87.
- (7) Iwai, L. K.; Luczynski, M. T.; Huang, P. H. Discoidin domain receptors: a proteomic portrait. *Cell. Mol. Life Sci.* **2014**, *71*, 3269–3279.
- (8) Borza, C. M.; Pozzi, A. Discoidin domain receptors in disease. *Matrix Biol.* **2014**, *34*, 185–192.
- (9) Kothiwale, S.; Borza, C. M.; Lowe, E. W., Jr.; Pozzi, A.; Meiler, J. Discoidin domain receptor 1 (DDR1) kinase as target for structure-based drug discovery. *Drug Discovery Today* **2015**, *20*, 255–261.
- (10) Ju, G. X.; Hu, Y. B.; Du, M. R.; Jiang, J. L. Discoidin domain receptors (DDRs): potential implications in atherosclerosis. *Eur. J. Pharmacol.* **2015**, *751*, 28–33.
- (11) Li, Y.; Lu, X.; Ren, X.; Ding, K. Small molecule discoidin domain receptor kinase inhibitors and potential medical applications. *J. Med. Chem.* **2015**, *58*, 3287–3301.
- (12) Avivi-Green, C.; Singal, M.; Vogel, W. F. Discoidin domain receptor 1-deficient mice are resistant to bleomycin-induced lung fibrosis. *Am. J. Respir. Crit. Care Med.* **2006**, *174*, 420–427.
- (13) Gao, M.; Duan, L.; Luo, J.; Zhang, L.; Lu, X.; Zhang, Y.; Zhang, Z.; Tu, Z.; Xu, Y.; Ren, X.; Ding, K. Discovery and optimization of 3-(2-(Pyrazolo[1,5-a]pyrimidin-6-yl)ethynyl)benzamides as novel selective and orally bioavailable discoidin domain receptor 1 (DDR1) inhibitors. *J. Med. Chem.* **2013**, *56*, 3281–3295.
- (14) Kim, H. G.; Tan, L.; Weisberg, E. L.; Liu, F.; Canning, P.; Choi, H. G.; Ezell, S. A.; Wu, H.; Zhao, Z.; Wang, J.; Mandinova, A.; Griffin, J. D.; Bullock, A. N.; Liu, Q.; Lee, S. W.; Gray, N. S. Discovery of a potent and selective DDR1 receptor tyrosine kinase inhibitor. *ACS Chem. Biol.* **2013**, *8*, 2145–2150.
- (15) Elkamhaw, A.; Park, J. E.; Cho, N. C.; Sim, T.; Pae, A. N.; Roh, E. J. Discovery of a broad spectrum antiproliferative agent with selectivity for DDR1 kinase: cell line-based assay, kinase panel, molecular docking, and toxicity studies. *J. Enzyme Inhib. Med. Chem.* **2016**, *31*, 158–166.

- (16) Richters, A.; Nguyen, H. D.; Phan, T.; Simard, J. R.; Grutter, C.; Engel, J.; Rauh, D. Identification of type II and III DDR2 inhibitors. *J. Med. Chem.* **2014**, *57*, 4252–4262.
- (17) Terai, H.; Tan, L.; Beauchamp, E. M.; Hatcher, J. M.; Liu, Q.; Meyerson, M.; Gray, N. S.; Hammerman, P. S. Characterization of DDR2 inhibitors for the treatment of DDR2 mutated non-small cell lung cancer. *ACS Chem. Biol.* **2015**, *10*, 2687–2696.
- (18) Murray, C. W.; Berdini, V.; Buck, I. M.; Carr, M. E.; Cleasby, A.; Coyle, J. E.; Curry, J. E.; Day, J. E.; Day, P. J.; Hearn, K.; Iqbal, A.; Lee, L. Y.; Martins, V.; Mortenson, P. N.; Munck, J. M.; Page, L. W.; Patel, S.; Roomans, S.; Smith, K.; Tamanini, E.; Saxty, G. Fragment-based discovery of potent and selective DDR1/2 inhibitors. *ACS Med. Chem. Lett.* **2015**, *6*, 798–803.
- (19) Day, E.; Waters, B.; Spiegel, K.; Alnadaf, T.; Manley, P. W.; Buchdunger, E.; Walker, C.; Jarai, G. Inhibition of collagen-induced discoidin domain receptor 1 and 2 activation by imatinib, nilotinib and dasatinib. *Eur. J. Pharmacol.* **2008**, *599*, 44–53.
- (20) Cowan-Jacob, S. W.; Fendrich, G.; Floersheimer, A.; Furet, P.; Liebetanz, J.; Rummel, G.; Rheinberger, P.; Centeleghe, M.; Fabbro, D.; Manley, P. W. Structural biology contributions to the discovery of drugs to treat chronic myelogenous leukaemia. *Acta Crystallogr., Sect. D: Biol. Crystallogr.* **2007**, *63*, 80–93.
- (21) Weisberg, E.; Manley, P. W.; Breitenstein, W.; Bruggen, J.; Cowan-Jacob, S. W.; Ray, A.; Huntly, B.; Fabbro, D.; Fendrich, G.; Hall-Meyers, E.; Kung, A. L.; Mestan, J.; Daley, G. Q.; Callahan, L.; Catley, L.; Cavazza, C.; Mohammed, A.; Neuberg, D.; Wright, R. D.; Gilliland, D. G.; Griffin, J. D. Characterization of AMN107, a selective inhibitor of native and mutant Bcr-Abl. *Cancer Cell* **2005**, *7*, 129–141.
- (22) O'Hare, T.; Shakespeare, W. C.; Zhu, X.; Eide, C. A.; Rivera, V. M.; Wang, F.; Adrian, L. T.; Zhou, T.; Huang, W. S.; Xu, Q.; Metcalf, C. A., 3rd; Tyner, J. W.; Loriaux, M. M.; Corbin, A. S.; Wardwell, S.; Ning, Y.; Keats, J. A.; Wang, Y.; Sundaramoorthi, R.; Thomas, M.; Zhou, D.; Snodgrass, J.; Commodore, L.; Sawyer, T. K.; Dalgarno, D. C.; Deininger, M. W.; Druker, B. J.; Clackson, T. AP24534, a pan-BCR-ABL inhibitor for chronic myeloid leukemia, potently inhibits the T315I mutant and overcomes mutation-based resistance. *Cancer Cell* **2009**, *16*, 401–412.
- (23) Canning, P.; Tan, L.; Chu, K.; Lee, S. W.; Gray, N. S.; Bullock, A. N. Structural mechanisms determining inhibition of the collagen receptor DDR1 by selective and multi-targeted type II kinase inhibitors. *J. Mol. Biol.* **2014**, *426*, 2457–2470.
- (24) Surry, D. S.; Buchwald, S. L. Dialkylbiaryl phosphines in Pd-catalyzed amination: a user's guide. *Chem. Sci.* **2011**, *2*, 27–50.
- (25) The assay was conducted by following the protocol from the agent manufacturer (<https://perkinelmerreagents.onconfluence.com>).
- (26) Fabian, M. A.; Biggs, W. H., 3rd; Treiber, D. K.; Atteridge, C. E.; Azimioara, M. D.; Benedetti, M. G.; Carter, T. A.; Ciceri, P.; Edeen, P. T.; Floyd, M.; Ford, J. M.; Galvin, M.; Gerlach, J. L.; Grotzfeld, R. M.; Herrgard, S.; Insko, D. E.; Insko, M. A.; Lai, A. G.; Lelias, J. M.; Mehta, S. A.; Milanov, Z. V.; Velasco, A. M.; Wodicka, L. M.; Patel, H. K.; Zarrinkar, P. P.; Lockhart, D. J. A small molecule-kinase interaction map for clinical kinase inhibitors. *Nat. Biotechnol.* **2005**, *23*, 329–336.
- (27) Matsuyama, W.; Wang, L.; Farrar, W. L.; Faure, M.; Yoshimura, T. Activation of discoidin domain receptor 1 isoform b with collagen up-regulates chemokine production in human macrophages: role of p38 mitogen-activated protein kinase and NF-kappa B. *J. Immunol.* **2004**, *172*, 2332–2340.
- (28) Nagase, T.; Uozumi, N.; Ishii, S.; Kita, Y.; Yamamoto, H.; Ohga, E.; Ouchi, Y.; Shimizu, T. A pivotal role of cytosolic phospholipase A (2) in bleomycin-induced pulmonary fibrosis. *Nat. Med.* **2002**, *8*, 480–484.
- (29) Colgrave, M. L.; Allingham, P. G.; Tyrrell, K.; Jones, A. Multiple reaction monitoring for the accurate quantification of amino acids: using hydroxyproline to estimate collagen content. *Methods Mol. Biol.* **2012**, *828*, 291–303.